



# Physiologically Based Pharmacokinetic Modeling of Cefadroxil in Mouse, Rat, and Human to Predict Concentration–Time Profile at Infected Tissue

Zhongxia Tan<sup>1</sup>, Youxi Zhang<sup>2</sup>, Chao Wang<sup>3</sup> and Le Sun<sup>1\*</sup>

<sup>1</sup>Department of Pharmaceutics, School of Pharmacy, China Medical University, Shenyang, China, <sup>2</sup>Department of Pharmacy, The Fourth Affiliated Hospital, China Medical University, Shenyang, China, <sup>3</sup>Liaoning Inspection Examination and Certification Centre, Shenyang, China

## OPEN ACCESS

### Edited by:

George D. Loizou,  
Health and Safety Executive,  
United Kingdom

### Reviewed by:

Jeffrey Fisher,  
ScitoVation, United States  
Jerry Campbell,  
Ramboll, United States

### \*Correspondence:

Le Sun  
lesun@cmu.edu.cn

### Specialty section:

This article was submitted to  
Predictive Toxicology,  
a section of the journal  
Frontiers in Pharmacology

Received: 09 April 2021

Accepted: 23 November 2021

Published: 23 December 2021

### Citation:

Tan Z, Zhang Y, Wang C and Sun L  
(2021) Physiologically Based  
Pharmacokinetic Modeling of  
Cefadroxil in Mouse, Rat, and Human  
to Predict Concentration–Time Profile  
at Infected Tissue.  
*Front. Pharmacol.* 12:692741.  
doi: 10.3389/fphar.2021.692741

The aim of this study was to develop physiologically based pharmacokinetic (PBPK) models capable of simulating cefadroxil concentrations in plasma and tissues in mouse, rat, and human. PBPK models in this study consisted of 14 tissues and 2 blood compartments. They were established using measured tissue to plasma partition coefficient ( $K_p$ ) in mouse and rat, absolute expression levels of hPEPT1 along the entire length of the human intestine, and the transporter kinetic parameters. The PBPK models also assumed that all the tissues were well-stirred compartments with perfusion rate limitations, and the ratio of the concentration in tissue to the unbound concentration in plasma is identical across species. These PBPK models were validated strictly by a series of observed plasma concentration–time profile data. The average fold error (AFE) and absolute average fold error (AAFE) values were all less than 2. The models' rationality and accuracy were further demonstrated by the almost consistent  $V_{ss}$  calculated by the PBPK model and noncompartmental method, as well as the good allometric scaling relationship of  $V_{ss}$  and  $CL$ . The model suggests that hPEPT1 is the major transporter responsible for the oral absorption of cefadroxil in human, and the plasma concentration–time profiles of cefadroxil were not sensitive to dissolution rate faster than  $T_{85\%} = 2$  h. The cefadroxil PBPK model in human is reliable and can be used to predict concentration–time profile at infected tissue. It may be useful for dose selection and informative decision-making during clinical trials and dosage form design of cefadroxil and provide a reference for the PBPK model establishment of hPEPT1 substrate.

**Keywords:** PBPK model, cefadroxil, hPept1,  $K_p$ , species extrapolation

## INTRODUCTION

Cefadroxil, a first-generation cephalosporin, has been commonly used in the treatment of different kinds of infections including urinary tract, skin, and respiratory infections (Tanrisever and Santella, 1986). Cefadroxil has a high bioavailability (Santella and Hennessy, 1982) despite its poor lipophilicity. It is a substrate of the peptide transporter PEPT1, and PEPT1 plays an important role in its intestinal absorption (Posada and Smith, 2013b). It is minimally metabolized in the body

and excreted primarily by the kidney, with over 90% of the administered dose being recovered in the urine intact within 24 h (Nightingale, 1980). The distribution of cefadroxil in the infected tissue is directly related to its pharmacological effects. Some tissue distribution data in human have been published (Nightingale, 1986; Akimoto et al., 1994; Nungu et al., 1995). However, they were only the concentration ratios of tissue/serum (plasma) at the peak time or other one time point. This did not reflect well the distribution of the drug in tissues.

The physiologically based pharmacokinetic (PBPK) model, a mechanistic quantitative framework, is established mainly based on physiological organ sizes, blood flow rates, tissue to plasma partition coefficient ( $K_p$ ), elimination mechanisms, etc. (Kesiosoglou et al., 2016). It can provide insight regarding drug concentration–time profiles in various tissues and build the relationship between dose and pharmacokinetic (PK) profiles in specific tissues to further assess the pharmacological effects. A number of PBPK models have been developed for assessing the clinical relevance of concentrations at target tissues, pharmacokinetic and pharmacodynamic relationship, *in vivo* pharmacokinetic properties of nanoparticles, the drug–drug interaction, etc. (Jones et al., 2015; Li et al., 2017). However, building an exact PBPK model needs to measure or calculate drug concentrations in various tissues, and this kind of data is very difficult to obtain in human.

$K_p$  is an important parameter in the PBPK model.  $K_p$  in human can be obtained by *in silico* method, such as Poulin method (Poulin and Theil, 2002), Berezhkovskiy method (Berezhkovskiy, 2004), and Rodgers and Rowland method (Rodgers et al., 2005). The tissues and plasma are assumed to be a combination of water, lipids, and proteins at pH = 7.4.  $K_p$  of tissues is mainly calculated based on the volume fraction of lipid, phospholipid, and water in tissue, unbound fraction of drug in tissue and plasma, and octanol/water partition coefficient ( $\log P$ ). *In silico* method can obtain the  $K_p$  values conveniently and quickly. However, it cannot consider the active diffusion of some drugs, for example, the distribution of the influx and efflux transporter involved.

$K_p$  also can be measured in animals, such as mouse and rat, then extrapolated to the  $K_p$  in human. A PBPK model describing and predicting terbinafine concentration in plasma and tissues in humans was established by supposing the identical  $K_p$  among mammals (Hosseini-Yeganeh and McLachlan, 2002). Chen et al. (2016) assumed that the ratio of the concentration in tissue to the unbound concentration in plasma is identical across species and then calculated the  $K_p$  in mouse, monkey, dog, and human based on  $K_p$  in rat and unbound fraction of deoxypodophyllotoxin in plasma of the corresponding species and rat. A PBPK-pharmacodynamic (PD) model linking to stomach to simultaneously predict vonoprazan PK and its antisecretory effects following administration to rats, dogs, and humans was developed (Kong et al., 2020). Due to a large species difference in free fraction of vonoprazan in the plasma ( $f_u$ ), the  $K_p$  in dog and  $K_p$  in human were calculated by  $f_u(\text{dog/human}) \times K_{p,\text{rat}}/f_{u,\text{rat}}$  based on the assumption that the ratios of tissue to plasma free concentration were identical across species (Kong et al., 2020), just like what Chen et al. (2016) did in their study.

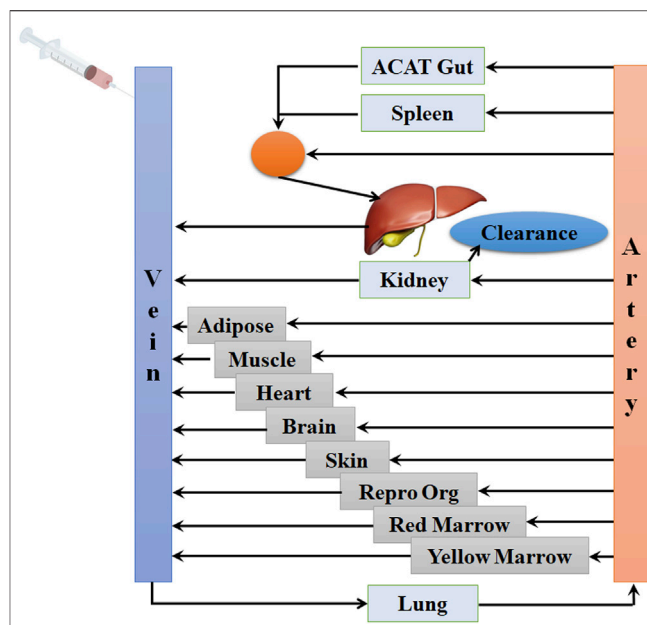


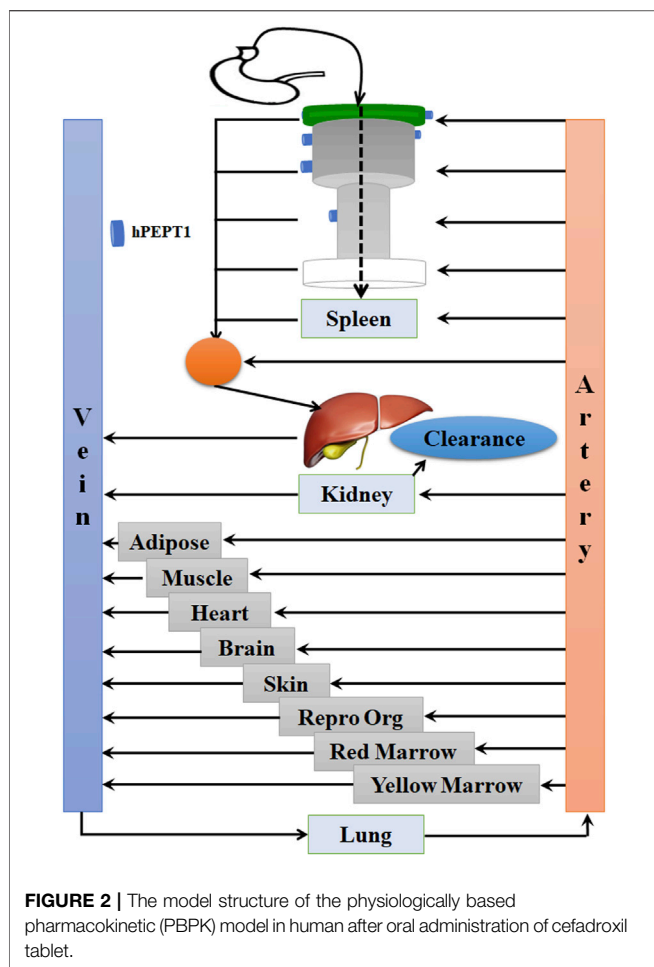
**FIGURE 1 |** The model structure of the physiologically based pharmacokinetic (PBPK) model in mouse and the PBPK model in rat after intravenous injection of cefadroxil solution.

Therefore, in this study, PBPK models were established to simulate the plasma and tissue concentration–time profiles in mouse and rat after intravenous injection of cefadroxil using the measured  $K_p$  in mouse and rat. After validating these models by *in vivo* data, a PBPK model in human was established to simulate the plasma and tissue concentration–time profile after oral administration using the  $K_p$  extrapolated from mouse and rat, as well as the absolute expression levels of hPEPT1 along the entire length of the human intestine and the transporter kinetic parameters.

## METHODS

### The Establishment of Physiologically Based Pharmacokinetic Models in Mouse, Rat, and Human

The PBPK model in mouse and PBPK model in rat simulating the plasma and other tissue concentration–time profiles after intravenous injection of cefadroxil solution were established, respectively. The PBPK model in human simulating the plasma and other tissues concentration–time profiles after oral administration of cefadroxil tablet was established based on the established PBPK models in mouse and rat. The PBPK models in mouse, rat, and human were established using GastroPlus™ (version 9.7, Simulation Plus, Lancaster, CA, USA). The default mouse, rat, and human fasted physiological models provided in GastroPlus™ were used. The model structure of PBPK model in mouse and PBPK model in rat after intravenous injection of cefadroxil solution



was shown in **Figure 1**. The model structure of PBPK model in human after oral administration of cefadroxil tablet was shown in **Figure 2**. The most common indications for cefadroxil are infection in the urinary tract and skin. The skin and kidney were both included in our models. The physiological parameters of PBPK models were shown in **Table 1**. The basic physicochemical and biopharmaceutical properties used in PBPK models were shown in **Table 2**. Over 90% of the cefadroxil is excreted unchanged in the urine within 24 h. Thus, the kidney was designed as the elimination organ.

The  $K_p$  values of lung, adipose, muscle, liver, spleen, heart, brain, kidney, skin, reproductive organ, red bone marrow, yellow bone marrow, and rest-of-body were shown in **Table 3**.  $K_p$  is one important parameter for PBPK model and reflects the distribution of the drug in various tissues. However, the  $K_p$  of human is difficult to obtain. Thus, it is commonly extrapolated from experimental animals. The ratio of the concentration in tissue to the unbound concentration in plasma is assumed identical across species. No literature published that there is a large species difference in free fraction in the plasma for cefadroxil. Thus, in this study, the  $K_p$  values in mouse, rat, and human are assumed to be the same. The observed  $K_p$  values in mice (Posada and Smith,

2013a) were measured by  $C_{\text{tissue}}/C_{\text{plasma}}$ . The  $C_{\text{tissue}}$  and  $C_{\text{plasma}}$  were collected at 20 min after 178 nmol/g oral doses of cefadroxil, since this time best represented the  $T_{\text{max}}$  of cefadroxil. The observed  $K_p$  values in rat were measured by  $AUC_{0-\infty, \text{tissue}}/AUC_{0-\infty, \text{plasma}}$  (Esumi et al., 1979) and  $C_{\text{tissue}}/C_{\text{plasma}}$  in steady state (Kim et al., 2014). The mean or median  $K_p$  values of lung, muscle, liver, spleen, heart, brain, and kidney in mice and rats were used in the PBPK models. The predicted  $K_p$  values were used for skin, red marrow, and yellow marrow. The  $K_p$  values of reproductive organ and rest of body were supposed as 0.5; the  $K_p$  value of adipose was supposed as 0.1 (**Table 3**).

About the PBPK model in human, the absorption scale factors (ASFs) calculated by Opt logD Model SA/V6.1 were used. The absolute expression contents of hPEPT1 in duodenum, jejunum 1, jejunum 2, ileum 1, ileum 2, and ileum 3 along the entire length of the human intestine were 16.28, 87.84, 73.93, 78.61, 63.41, and 49.29 mg, respectively (Groer et al., 2013; Drozdziak et al., 2014; Sun et al., 2018). These values were measured by liquid chromatography-tandem mass spectrometry (LC-MS/MS) and had been successfully used in our other PBPK model for valacyclovir (Sun et al., 2018). The hPEPT1 expressions of the cecum and colon were adjusted to zero. The values of  $K_m$  and  $V_{\text{max}}$  were 860.31 mg/L and 0.0025  $\mu\text{g/s/mg-hPEPT1}$ , respectively. They are the values corresponding to the hPEPT1-mediated transport of cefadroxil inputted into the model. The  $K_m$  was measured by *in situ* single-pass intestinal perfusion in huPEPT1 mice with cefadroxil concentration in perfusate buffer that varied from 0.01 to 25 mM in the literature (Hu and Smith, 2016). The  $V_{\text{max}}$  ( $0.056 \pm \text{nmol/s/cm}^2$ ) was optimized when establishing the model.

## Model Validation

The PBPK model in mice was used to simulate the plasma concentration–time profiles following intravenous injection of 11, 44.5, and 528 nmol/g cefadroxil. Then, the simulated profiles were validated by the observed concentration–time profiles (Posada and Smith, 2013a; Hu and Smith, 2016). The observed data were obtained by the following method. The wild-type mice were given 11, 44.5, and 528 nmol/g body weight (*BW*) [ $^3\text{H}$ ]cefadroxil by intravenous bolus injection. Serial blood samples were collected at 1, 2.5, 5, 10, 20, 30, 45, 90, and 120 min after dosing *via* tail transections. The cefadroxil in the plasma samples was measured using a dual-channel liquid scintillation counter (Posada and Smith, 2013a; Hu and Smith, 2016).

The PBPK model in rat was used to simulate the plasma concentration–time profiles of cefadroxil following intravenous injection of 2 mg/kg. Then, the simulated profile was validated by the observed concentration–time profile (Jin et al., 2014; Kim et al., 2014). The observed data were obtained by the following method. The rats were administered intravenous cefadroxil (2 mg/ml in phosphate-buffered saline) at a dose of 2 mg/kg. Blood samples were taken from the femoral artery cannula at 0, 5, 15, 30, 60, 90, 120, 180, and 240 min after dosing. The cefadroxil in the plasma samples was measured by LC-MS/MS (Jin et al., 2014; Kim et al., 2014).

**TABLE 1** | Physiological parameters of PBPK models in mouse, rat, and human.

Tissues	Mouse		Rat		Human	
	Volume (ml)	The blood flow (ml/s)	Volume (ml)	The blood flow (ml/s)	Volume (ml)	The blood flow (ml/s)
Lung	0.15833	0.11347	2.604	0.9389	1,125.5	98.1779
Arterial supply	0.57	0.11347	6.944	0.9389	2,148.17	98.1779
Venous return	1.13	0.11347	14.012	0.9389	4,296.34	98.1779
Adipose	1.91048	0.00127	12.4	0.00784	24,307.3	8.09433
Muscle	9.2219	0.01517	151.28	0.14695	25,174.7	12.5874
Liver	1.66355	0.03352	12.772	0.23111	1,590.1	24.3444
ACAT gut	—	0.02498	—	0.14689	—	12.263
Spleen	0.10081	0.0015	0.744	0.01175	169.973	2.83294
Heart	0.10922	0.00467	1.488	0.07638	337.26	4.10344
Brain	0.41647	0.00759	1.53402	0.02554	1,493.16	12.6919
Kidney	0.38929	0.0213	4.588	0.18019	360.411	22.1051
Skin	3.51582	0.01009	49.6	0.11361	2,831.73	5.66346
ReproOrg	0.148	0.00049	3.1	0.00979	50.6174	0.17716
Red marrow	0.83204	0.01355	2.31146	0.03568	1,106.48	5.53242
Yellow marrow	0.52449	0.00085	5.14347	0.00794	3,075.64	1.53782
RestOfBody	1.3735	0.00497	30.282	0.10386	2,681.07	1.34054

**TABLE 2** | Physicochemical and biopharmaceutical properties of cefadroxil used in the PBPK models.

Input parameter	PBPK model in mouse	PBPK model in rat	PBPK model in human
Molecular weight		363.39 <sup>a</sup>	
Log <i>P</i>		−0.4 <sup>a</sup>	
<i>pK</i> <sub>a</sub>		9.71 (acid), 7.21 (base), 2.55 (acid) <sup>b</sup>	
Solubility (mg/ml @pH = 5.15)		12.44 <sup>c</sup>	
Blood/plasma conc. ratio		1	
Use Exp Plasma Fup (%)		71.9 <sup>a</sup>	
Mean precipitation time (s)		900 <sup>d</sup>	
Diffusion coefficient (cm <sup>2</sup> /s × 10 <sup>5</sup> )		0.75 <sup>d</sup>	
Drug particle density (g/ml)		1.2 <sup>d</sup>	
Dose (mg)	0.1, 0.4, 4.79	0.62	375.5, 1,126.5, 2,253
Formulation option	IV: Bolus	IV: Bolus	IR: Suspension
Passive <i>P</i> <sub>eff</sub> (cm/s × 10 <sup>4</sup> )			0.03 <sup>d</sup>
<i>V</i> <sub>ss</sub> (L)	0.012	0.159	24.747
Clearance (L/h)	Kidney : 0.031 <sup>e</sup>	Kidney : 0.18 <sup>e</sup>	Kidney : 8.50 <sup>e</sup>

<sup>a</sup>Drugbank.

<sup>b</sup>Shalaeva et al., 2008.

<sup>c</sup>Shoghi et al., 2013.

<sup>d</sup>Default value in GastroPlus™.

<sup>e</sup>Optimizing value based on observed plasma concentration–time curve.

The PBPK model in human was used to simulate the plasma concentration–time profiles following oral administration of 5, 15, and 30 mg/kg cefadroxil. Then, the simulated profiles were validated by the observed concentration–time profiles (Garrigues et al., 1991). The observed data were obtained by the following method. Cefadroxil was given orally to the 6 volunteers in doses of 5 and 15 mg/kg. Three of the volunteers also received 30 mg/kg. Blood was taken at 0, 10, 20, 30, 45, 60, 75, 90, 120, 180, 240, 360, and 480 min after dosing. Cefadroxil was assayed by high-performance liquid chromatography within 4 days (Garrigues et al., 1991).

Cefadroxil is well absorbed on oral administration; the fraction of cefadroxil dose absorbed was nearly 100%. In addition, the elimination phase of oral administration and intravenous

injection should be consistent. Thus, concentrations of cefadroxil in plasma, kidney, muscle, spleen, heart, lung, liver, and brain of rats following 25 and 100 mg/kg intravenous injection were simultaneously predicted, and the prediction was validated by observed data at 1 and 3 h in rats after oral administration of 25 and 100 mg/kg (Esumi et al., 1979). Simulating the oral absorption process requires membrane permeability in rat and others' data; this brings a lot of uncertainties to the PBPK model. The establishment of the PBPK model in rats in this study is to provide reliable distribution and elimination data for the human PBPK model. The intravenous injection model is conducive to obtaining accurate distribution and elimination data. Therefore, the PBPK model in rat was established to simulate intravenous

**TABLE 3** | Summary of cefadroxil  $K_p$  values.

Tissue	Predicted $K_p$ values by lukacova (Rodgers-single) method using GastroPlus™	Observed $K_p$ values in mice (Posada and Smith, 2013a)	Observed $K_p$ values in rats (Esumi et al., 1979)	Observed $K_p$ values in rats (Kim et al., 2014)	The $K_p$ values used in PBPK models
Lung	1.71	0.60	0.44		0.52
Adipose	0.25				0.1
Muscle	0.87	0.32	0.18		0.25
Liver	1.82	2.14	0.81	0.37	0.81
Spleen	1.42	0.35	0.47		0.41
Heart	1.17	0.20	0.24	0.24	0.23
Brain	0.54		0.11	0.12	0.11
Kidney	2.01	7.03	6.72	15.4	6.87
Skin	0.89				0.89
Reproductive organ	2.02				0.5
Red marrow	0.47				0.47
Yellow marrow	0.25				0.25
Rest of body	1.43				0.5

injection, and the prediction was validated by the observed data at the elimination phase.

The fold error (FE), average fold error (AFE), and absolute average fold error (AAFE) were calculated as follows:

$$FE = \frac{\text{Predicted}_i}{\text{Observed}_i} \quad (1)$$

$$AFE = 10^{\frac{1}{n} \sum \log \left( \left| \frac{\text{Predicted}_i}{\text{Observed}_i} \right| \right)} \quad (2)$$

$$AAFE = 10^{\frac{1}{n} \sum \left| \log \left( \frac{\text{Predicted}_i}{\text{Observed}_i} \right) \right|} \quad (3)$$

where  $\text{Predicted}_i$  is the predicted concentration at time point  $i$ ,  $\text{Observed}_i$  is the observed concentration at time point  $i$ , and  $n$  is the number of time points at which the concentration was determined. The FE indicates the predictive accuracy of each data point, as shown in Eq. 1. The AFE indicates whether the predicted profile underestimates or overestimates the observed values, as shown in Eq. 2. The AAFE quantifies the absolute error from the observed values, as shown in Eq. 3. If the FE of all the data points is between 0.3 and 3 (within 3-fold error) and the AFE and AAFE are both less than 2, it can be considered as a successful simulation.

## Ethics

The *in vivo* human data and animal data used in this article were all cited from references. Thus, the ethical review process was not needed in this study and was not provided.

## Parameter Sensitivity Analysis

Parameter sensitivity analysis (PSA) was performed using PBPK model in human to find out the key factors that influenced the simulated cefadroxil plasma concentration–time profile. The initial input values were varied in the range of 0.1–10 times to allow 10-fold range increase and decrease.  $C_{\max}$  and  $AUC_{0-\infty}$  of cefadroxil were then evaluated at each of the input values for each of the parameters studied.

## Model Application

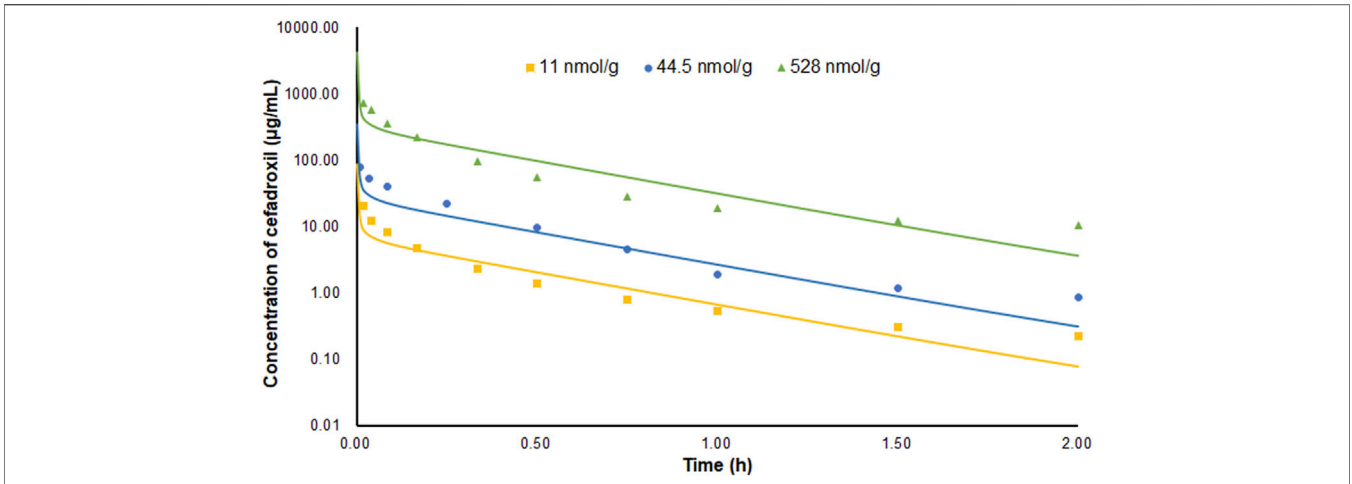
The PBPK model in human was used to quantitatively evaluate the effect of hPEPT1 on the oral absorption of cefadroxil after its predictive performance had been fully validated. The fraction of cefadroxil dose absorbed was simulated in both the absence and presence of hPEPT1 expression in the intestine.

The validated PBPK model in human was also used to quantitatively evaluate the effect of dissolution rate on the oral absorption of cefadroxil. The simulated plasma concentration–time profiles of cefadroxil were obtained, respectively, at different dissolution rates ( $T_{85\%} = 0.5, 1, 1.5, 2, 4, 6$  h). The simulated plasma concentration–time profile obtained by input  $T_{85\%} = 0.5$  dissolution rate [ $> 85\%$  solubility (pH 1.2–6.8) in 0.5 h; “very rapid dissolution”] was used as the reference, then it was used to compare with those obtained by inputting other dissolution rates.

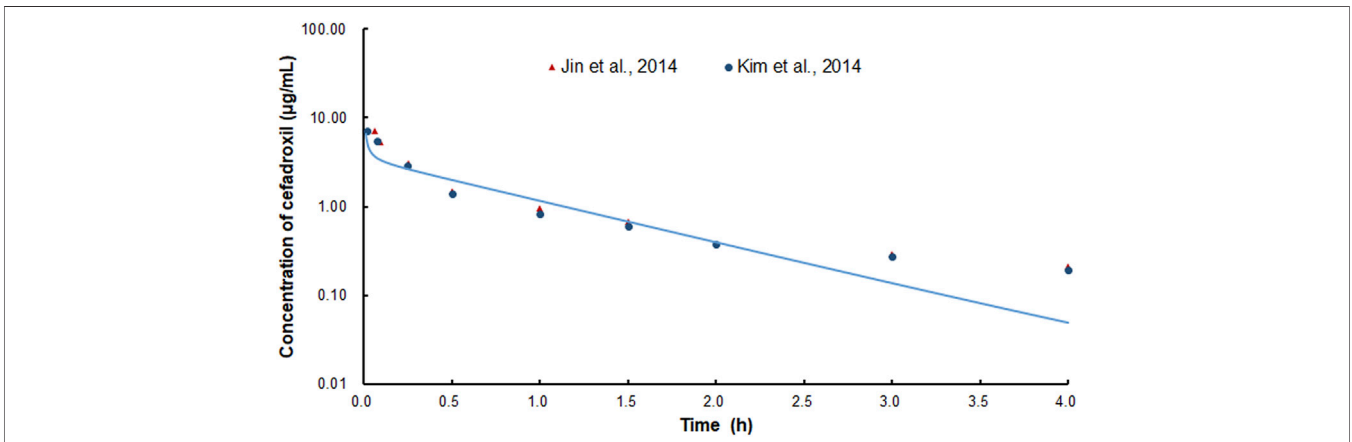
## RESULTS

### The Physiologically Based Pharmacokinetic Models in Mouse, Rat, and Human

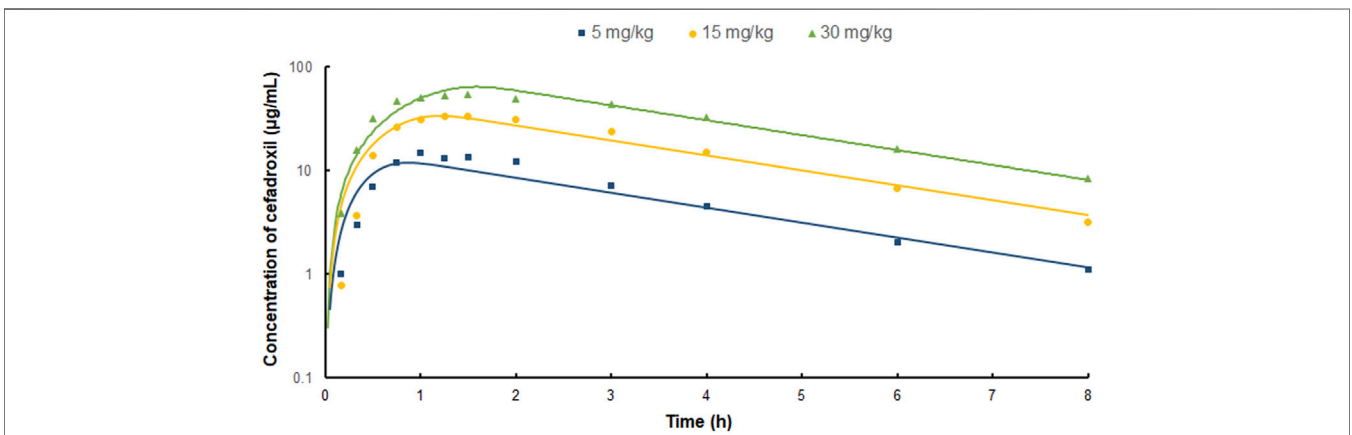
The predicted and observed plasma concentrations of cefadroxil obtained from the PBPK models in mouse, rat, and human are present in Figure 3, Figure 4, and Figure 5. As shown in the above Figures, the observed and predicted plasma concentration–time profiles superimposed. The predicted and observed values of  $C_{\max}$  and  $AUC_{0-\infty}$  after each dose administration of cefadroxil to mouse, rat, and human are shown in Table 4. The predicted values and observed values are close. The models in mouse, rat, and human were all validated by FE. Most of the FE values were within 2-fold error (Figure 6), but there were two outliers. The FE value of data point at 0.17 h of model in human simulating 15 mg/kg was without 3-fold error (FE = 5.76). The FE value of data point at 4 h of model in rat was without 3-fold error (FE = 0.25). These may be caused by errors in the blood sampling or detection for the first and the last time



**FIGURE 3 |** Predicted and observed plasma concentration–time profiles of cefadroxil in mice after intravenous injection of 11, 44.5, and 528 nmol/g (n = 6–8).



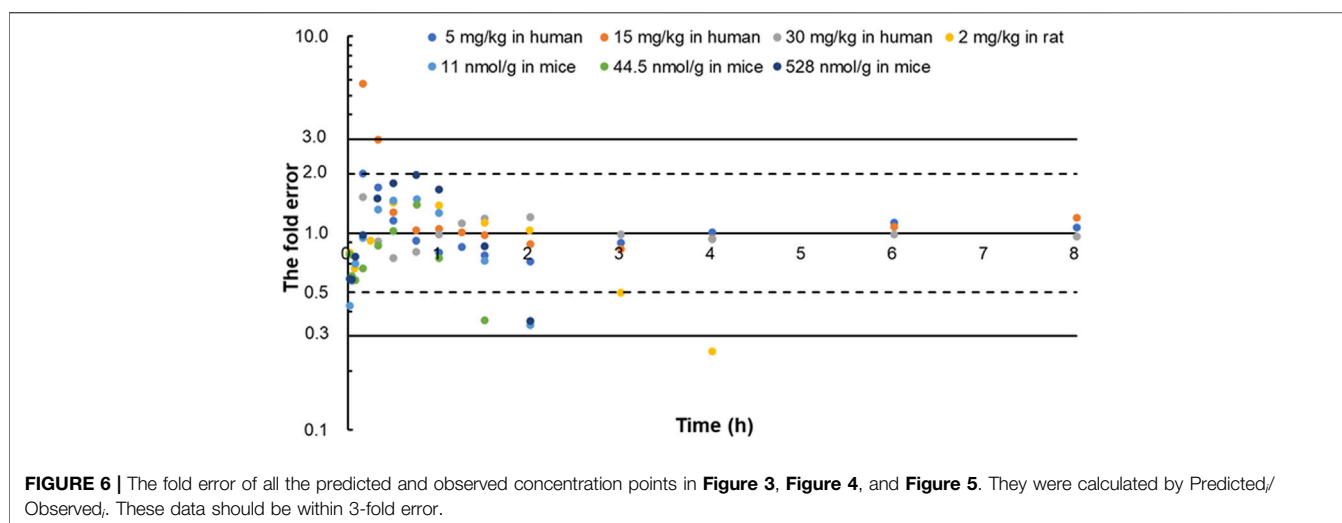
**FIGURE 4 |** Predicted and observed plasma concentration–time profiles of cefadroxil in rats after intravenous injection of 2 mg/kg (n = 4–5).



**FIGURE 5 |** Predicted and observed plasma concentration–time profiles of cefadroxil in human after oral administration of 5, 15, and 30 mg/kg (n = 3).

**TABLE 4** | The predicted and observed values of  $C_{max}$  and  $AUC_{0-\infty}$  after each dose administration of cefadroxil to mouse, rat, and human.

Species	Dose (mg)	Dosing route	$C_{max}$ ( $\mu\text{g/ml}$ )		$AUC_{0-\infty}$ ( $\mu\text{g}\cdot\text{h/ml}$ )	
			Predicted	Observed	Predicted	Observed
Mouse	0.1	IV			3.17	3.79
	0.4	IV			12.69	18.91
	4.79	IV			151.98	169.97
Rat	0.62	IV			3.42	4.04
Human	375.5	Oral	12.07	14.69	44.14	49.15
	1,126.5	Oral	34.28	33.88	132.37	133.96
	2,253	Oral	64.43	53.82	264.50	264.5

**FIGURE 6** | The fold error of all the predicted and observed concentration points in **Figure 3**, **Figure 4**, and **Figure 5**. They were calculated by Predicted/Observed. These data should be within 3-fold error.

point. The AFE and AAFE values for models in mouse, rat, and human were all less than 2. It indicates an adequate fitting, and the PBPK models in mouse, rat, and human are accurate and reliable.

The predicted and observed plasma/tissue concentrations were shown in **Figure 7**. The predicted concentrations of plasma and tissues at 0.5 h were all higher than the observed data. This was because the administration method of prediction was intravenous injection, but observed data were obtained by oral administration. The concentrations at the elimination phase were validated by the observed value. The FEs of 1 and 3 h were shown in **Figure 7I**. There were three points without 3-fold error. One was the point at 1 h in brain (FE = 7.25). This may be caused by the existing blood–brain barrier for cefadroxil. There were not observed data for 25 mg/kg in brain in the literature because they were not detected. Two of them were the points of 25 and 100 mg/kg at 1 h in muscle (FE = 5.44, FE = 4.16). This may be caused by different methods of administration or other reasons.

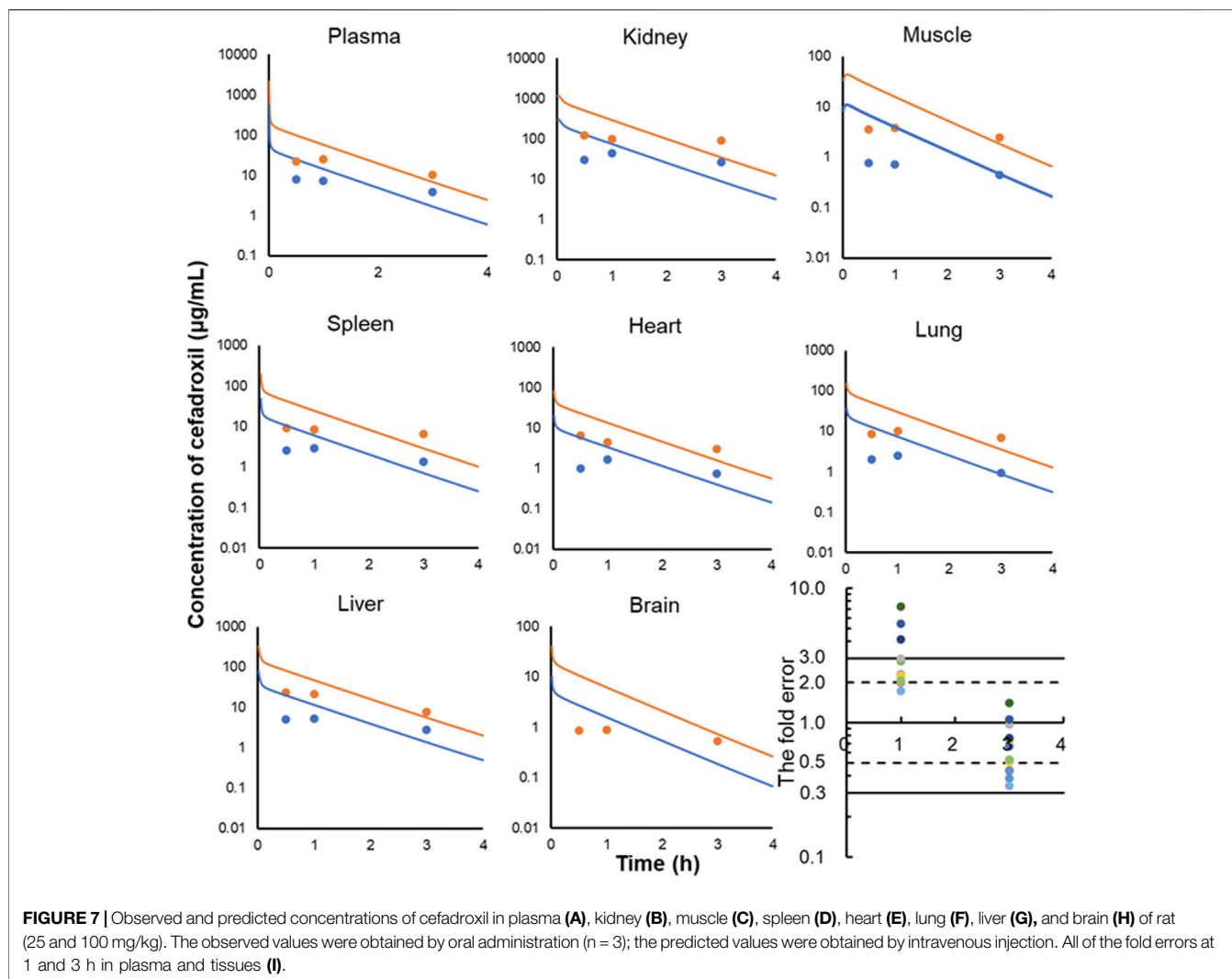
The  $V_{ss}$  calculated by the PBPK model is based on the  $K_p$  and volume of tissues. The  $V_{ss}$  values of mouse, rat, and human were 0.012, 0.159, and 23.25 L. They are almost identical with the values published in the observed PK articles (0.012 L in mouse, 0.26 L in rat) (Kim et al., 2014; Hu and Smith, 2016). The  $V_{ss}$  and

$CL$  used in the PBPK model required an allometric scaling relationship with  $BW$  ( $Y = a \times BW^b$ ) ( $R^2$  of  $V_{ss} = 0.9993$ ,  $R^2$  of  $CL = 1$ ), as shown in **Figure 8**. The estimated slopes (a) for  $V_{ss}$  and  $CL$  were 0.4288 and 0.4108. The scaling exponent (b) for  $V_{ss}$  is equal to 0.9476. The value for  $CL$  is 0.7012. The rational  $V_{ss}$  and good allometric scaling relationship further verify the reliability of PBPK models in this study.

The predicted tissues and plasma concentrations of cefadroxil after oral dosing 15 mg/kg obtained from the PBPK model in human were shown in **Supplementary Figure S1** and **Supplementary Table S1**. The  $C_{max}$  of lung, plasma, adipose, muscle, liver, spleen, heart, brain, kidney, and skin was 17.8, 34.23, 3.4, 8.33, 33.37, 14.05, 7.88, 3.77, 210.22, and 29.79  $\mu\text{g/ml}$ , respectively. The  $C_{max}$  was highest in the kidney and lowest in adipose and brain. The  $T_{max}$  of muscle and liver was 1.5 and 1 h, respectively; for other tissues, 1.25 h.

## Parameter Sensitivity Analysis

As shown in **Figures 9A and B**, PSA suggested that the predicted  $C_{max}$  of cefadroxil was most sensitive to changes in muscle  $K_p$ . It was also sensitive to changes in  $K_p$  of kidney, adipose, and liver. The changes in  $K_p$  values almost do not cause the changes in  $AUC_{0-\infty}$ . As shown in **Figures 9C and D**, PSA indicated that the predicted  $C_{max}$  and  $AUC_{0-\infty}$  of cefadroxil were sensitive to



changes in clearance in kidney and  $V_{\max}$  of hPEPT1. However, they were insensitive to passive permeability and solubility of cefadroxil.

### Effect of hPEPT1 on the Oral Absorption of Cefadroxil

The simulated fractions of cefadroxil dose absorbed in the absence and presence of hPEPT1 intestinal expression are shown in **Figure 10**. The fraction of cefadroxil dose absorbed was 7.8% in the absence of hPEPT1 and 99.9% in the presence of hPEPT1. As shown in **Figure 11A**, there is a good correlation between the absolute expression quantity of hPEPT1 in human and cefadroxil effective permeability in wild-type mouse duodenum, jejunum, ileum, and colon. The humans and mice have large absorption at duodenum, jejunum, and ileum, but their absorptions at colon were both small. The passive permeability used in the PBPK model in human and effective permeability of cefadroxil in PepT1 knockout mice were shown in **Figure 11B**. The values were both much less than the absorption through hPEPT1.

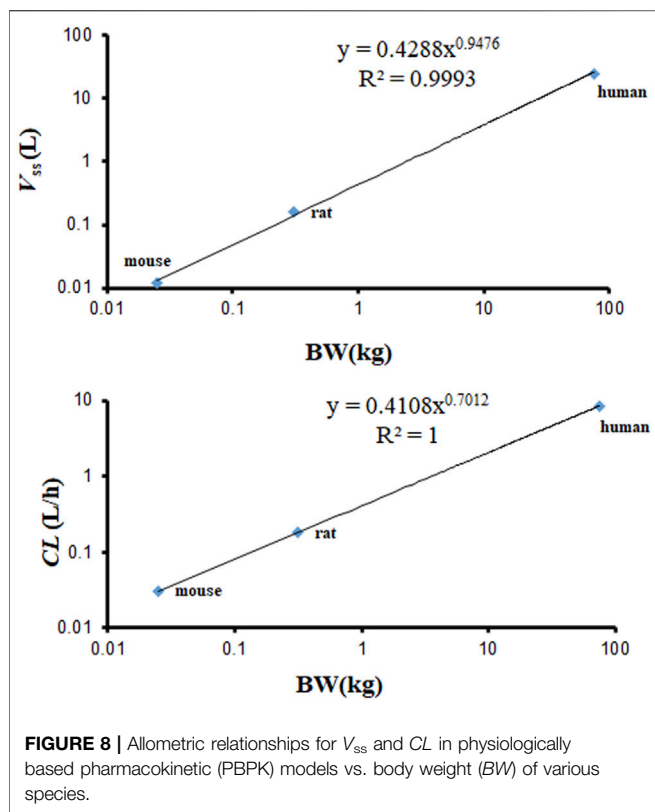
### Effect of Drug Release Rate on the Oral Absorption of Cefadroxil

The predicted plasma concentration–time profiles of cefadroxil when using different dissolution rates are shown in **Supplementary Figure S2**. The relative errors of  $C_{\max}$  and  $AUC_{0-\infty}$  were within 20% up to  $T_{85\%} = 2$  h. This indicated that the  $C_{\max}$  and  $AUC_{0-\infty}$  were not sensitive to dissolution rate when the dissolution rate was not slower than  $T_{85\%} = 2$  h.

## DISCUSSION

### The $K_p$ Values Used in the Physiologically Based Pharmacokinetic Models

As shown in **Table 3**, there are some discrepancies between predicted  $K_p$  values in human and observed values in mouse and rat, especially for kidney. Cefadroxil was excreted primarily by the kidney, with over 90% of the administered dose being recovered in the urine intact within 24 h. PEPT2 (SLC15A2) mediates the



renal reabsorption of cefadroxil (Xie et al., 2016). The predicted method cannot consider this factor and led to the discrepancy. The observed  $K_p$  values in mouse and rat are closer to most tissues.

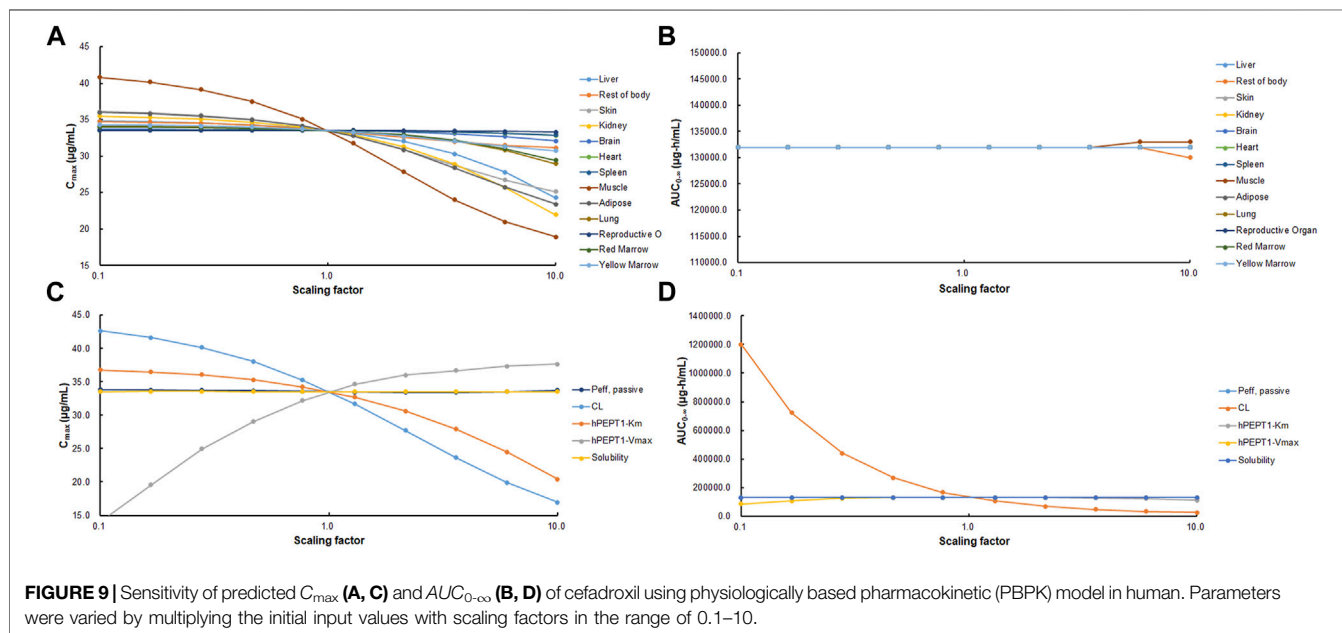
The incomplete observed tissue distribution data in human were collected as below. The mean cefadroxil concentration ratios of gingiva/serum and mandibular bone/serum at the peak time

were 0.54 and 0.21 (Akimoto et al., 1994). The concentrations of cefadroxil in saliva 3–4 h after drug administration were 40%–112% of those found in serum. The peak concentrations of cefadroxil in pleural fluid after a single 1-g dose of cefadroxil in 4 patients were about 50% of those found in serum. The peak concentration of cefadroxil in lung tissue was 54%–69% of the serum value (Nightingale, 1986). The mean value of  $C_{bone}/C_{plasma}$  at the same time from administration was 0.3 (Nungu et al., 1995). The peak concentration of cefadroxil in skin blister was 20 mg/L after 3 h. The peak concentration of cefadroxil in serum was 28.4 mg/L after 1.5 h (Simon et al., 1980). The cefadroxil tissue concentrations in hepatobiliary tissues were roughly parallel of those seen in plasma (Palmu et al., 1980). The  $K_p$  values of tissues used in PBPK model were almost consistent with these observed distribution data in human. This further validated the reliability of  $K_p$  values used in the PBPK models and the reasonability of the PBPK models in this study.

### Parameter Sensitivity Analysis

Muscle tissue accounted for 33.52% of the  $BW$  and had relatively high blood flow. This induced that  $C_{max}$  of cefadroxil was most sensitive to changes in muscle  $K_p$ . Adipose accounted for 32.37% of  $BW$ , so it also affected the  $C_{max}$  of cefadroxil. Kidney and liver were quick blood perfusion organs; besides, the kidney was the elimination organ in this study. Therefore, the  $C_{max}$  of cefadroxil was sensitive to changes in their  $K_p$ . For these four tissues and organs, the observed and reasonable  $K_p$  values were used in this study. Though the  $C_{max}$  and  $AUC_{0-\infty}$  of cefadroxil were not sensitive to some tissue  $K_p$  values, the tissue  $K_p$  values were important to assess the distribution of the drug in the tissues.

The solubilities of cefadroxil in water from pH 3 to 6.88 were added in the PBPK models (Shoghi et al., 2013). Cefadroxil was quite soluble among these pH values, so its  $C_{max}$  and  $AUC_{0-\infty}$  values were insensitive to solubility. Abundant hPEPT1 expressed along the intestine plays a major role in the absorption of



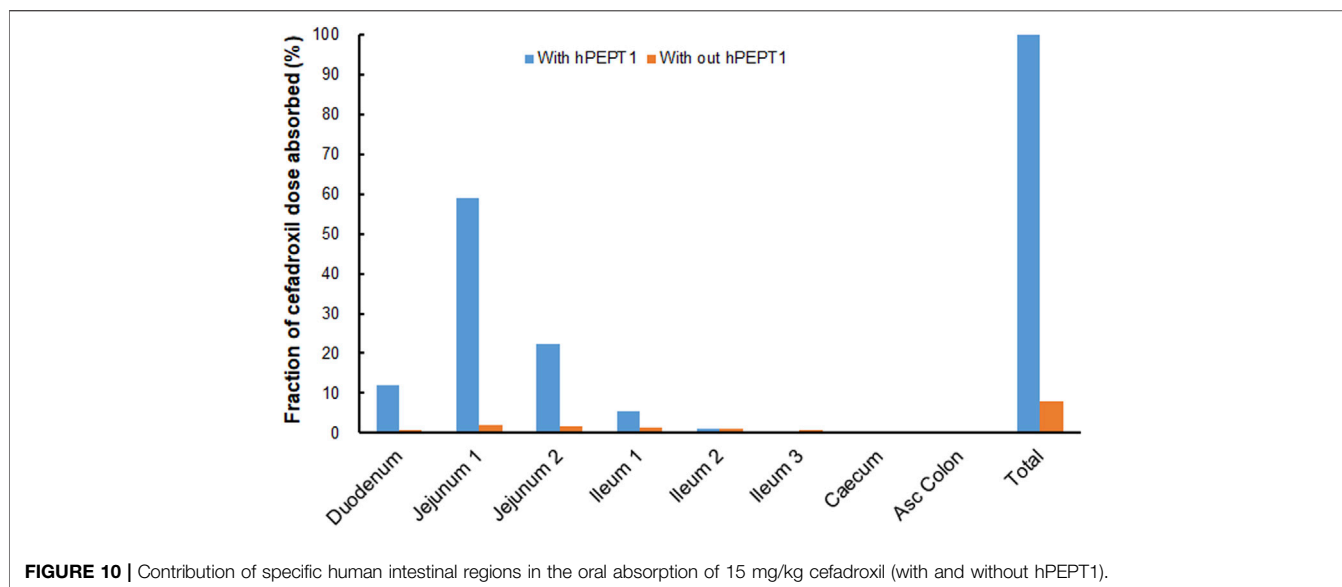


**FIGURE 10** | Contribution of specific human intestinal regions in the oral absorption of 15 mg/kg cefadroxil (with and without hPEPT1).

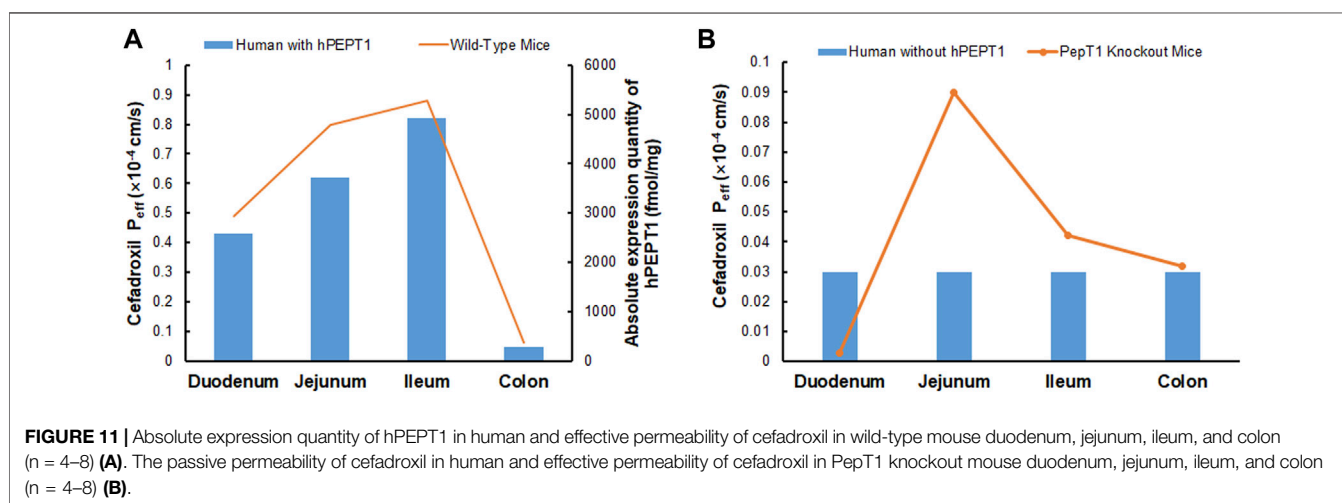


**FIGURE 11** | Absolute expression quantity of hPEPT1 in human and effective permeability of cefadroxil in wild-type mouse duodenum, jejunum, ileum, and colon (n = 4–8) (A). The passive permeability of cefadroxil in human and effective permeability of cefadroxil in PepT1 knockout mouse duodenum, jejunum, ileum, and colon (n = 4–8) (B).

cefadroxil. This makes the  $C_{max}$  and  $AUC_{0-\infty}$  values insensitive to passive permeability but sensitive to  $V_{max}$  of hPEPT1.

## Model Calibration

The clearances in the PBPK models of mouse, rat, and human in this study were obtained by optimizing the value based on observed plasma concentration–time curves. For the PBPK model of mouse and human, the calibrations were both based on one dosage and validated by the other two dosages. For the PBPK model of rat, the calibration was based on one dosage. The  $K_p$  values of adipose, reproductive organ, and rest of body were calibrated based on the predicted  $K_p$  values using GastroPlus™, observed plasma concentration–time curves, and experience. The  $V_{ss}$  values calculated by PBPK models were almost identical with the values published in the observed PK articles. The  $V_{ss}$  and  $CL$  values among the three species were in the good allometric scaling relationship. These all indicated the reasonability of the calibration.

## Effect of hPEPT1 on the Oral Absorption of Cefadroxil

The fraction of cefadroxil dose absorbed decreased from 99.9% to 7.8% when the simulations were performed without hPEPT1. Cefadroxil was absorbed completely with hPEPT1 among these three dosages when simulating using PBPK model in human in this study. PepT1 ablation resulted in 23-fold reductions in peak plasma concentrations and 14-fold reductions in systemic exposure of cefadroxil after oral dosing in wild-type and PepT1 knockout mice (Posada and Smith, 2013b). These both demonstrated that PepT1 is the major transporter responsible for the oral absorption of cefadroxil.

## Effect of Drug Release Rate on the Oral Absorption of Cefadroxil

The  $C_{max}$  and  $AUC_{0-\infty}$  of cefadroxil were insensitive to the dissolution rate up to  $T_{85\%} = 2$  h because of the high

solubility of cefadroxil. When the dissolution rates were slower than  $T_{85\%} = 2$  h, more drug would be released at the lower segment of the intestine, where the expression of hPEPT1 is smaller. This induces to a decrease in oral absorption of cefadroxil. In order to reduce administration times per day and increase patient compliance, cefadroxil was often designed as a sustained-release dosage form. This study suggested that attention should be paid to the oral absorption of cefadroxil when the release rate of its formulation is too slow.

## The Limitations of This Study

There are some limitations of this study due to the assumptions and data sources. The plasma protein-binding data obtained from Drugbank database were used in PBPK models of all the species in this study. The data in each species were not found. There may exist in the blood–brain barrier for cefadroxil, but it was not considered due to lack of data.

Cefadroxil is a substrate of PEPT2 (SLC15A2), and PEPT2 mediates the renal reabsorption of cefadroxil (Xie et al., 2016). The renal clearances of mouse, rat, and human were 0.52, 3.00, and 141.67 ml/min in this study. They were slightly higher than the glomerular filtration rates (GFRs) of these three species (mouse: about 0.30 ml/min, rat: about 2.38 ml/min, human: about 125 ml/min), indicating that there may be reabsorption and active secretion. These were complicated and were not considered in the PBPK models in the study, instead just the *CL* was added in the kidney. For cefadroxil, there was no evidence of its nonlinear intestinal absorption in mice (Posada and Smith, 2013a). However, there was an increase in plasma clearance as the dose increases in rat. This phenomenon was attributed to a saturable renal tubular reabsorption (Garcia-Carbonell et al., 1993). The PK behavior of cefadroxil was dose-dependent in human, too. This phenomenon was the result of the combined action of saturable active gastrointestinal absorption (PEPT1) and saturable renal tubular reabsorption of cefadroxil (PEPT2) (Garrigues et al., 1991). The PBPK models in this study considered the PEPT1, but did not consider the PEPT2, thus this no-linear phenomenon was not found in rat and human in our PBPK models.

## CONCLUSION

In the present study, the PBPK models in mouse, rat, and human simulating the plasma and tissue concentration–time profiles of cefadroxil were established successfully and validated strictly by the observed PK data. The models' rationality and accuracy were further demonstrated by the almost consistent  $V_{ss}$  calculated by different methods, good allometric scaling relationship of  $V_{ss}$  and *CL*, and model PSA. The PBPK model in human suggested that hPEPT1 was the major transporter responsible for the oral absorption of cefadroxil in human. It also suggested that the plasma concentration–time profile of cefadroxil was not sensitive to dissolution rate faster than  $T_{85\%} = 2$  h. All in all, the PBPK model in human may be useful for dose selection and informative

decision-making during clinical trials and dosage form design of cefadroxil and provide a reference for the PBPK studies of hPEPT1 substrate.

## DATA AVAILABILITY STATEMENT

The original contributions presented in the study are included in the article/**Supplementary Material**, further inquiries can be directed to the corresponding author.

## ETHICS STATEMENT

Ethical approval was not provided for this study on human participants because the human data used in this study were all cited from references. Thus, the ethical review process was not needed and was not provided. Written informed consent was not provided because the human data used in this study were all cited from references. We did not conduct any human subject research by ourselves. Thus, the written informed consent was not provided. Ethical review and approval were not required for the animal study because the animal data used in this article were all cited from references. Thus, the ethical review process was not needed in this study and was not provided.

## AUTHOR CONTRIBUTIONS

Participated in research design: YZ, CW, and LS. Conducted the experiments: ZT and LS. Wrote or contributed to the writing of the article: ZT and LS.

## FUNDING

This work was supported by the National Natural Science Foundation of China (No. 81603055) and National Natural Science Foundation of China (No. 81703447).

## SUPPLEMENTARY MATERIAL

The Supplementary Material for this article can be found online at: <https://www.frontiersin.org/articles/10.3389/fphar.2021.692741/full#supplementary-material>

**Supplementary Figure S1** | Predicted tissues and plasma concentration-time profiles of cefadroxil in human after oral administration 15 mg/kg. The dots were the observed data in plasma.

**Supplementary Figure S2** | The effect of release rate on the simulated plasma concentration-time profiles of cefadroxil after oral administration of 15 mg/kg cefadroxil in human.

**Supplementary Table S1** | The predicted tissues and plasma concentrations of cefadroxil after oral dosing 15 mg/kg obtained from the PBPK model in human in this study.

## REFERENCES

- Akimoto, Y., Komiya, M., Kaneko, K., and Fujii, A. (1994). Cefadroxil Concentrations in Human Serum, Gingiva, and Mandibular Bone Following a Single Oral Administration. *J. Oral Maxillofac. Surg.* 52 (4), 397–401. doi:10.1016/0278-2391(94)90447-2
- Berezhkovskiy, L. M. (2004). Volume of Distribution at Steady State for a Linear Pharmacokinetic System with Peripheral Elimination. *J. Pharm. Sci.* 93 (6), 1628–1640. doi:10.1002/jps.20073S0022-3549(16)31526-X
- Chen, Y., Zhao, K., Liu, F., Xie, Q., Zhong, Z., Miao, M., et al. (2016). Prediction of Deoxypodophyllotoxin Disposition in Mouse, Rat, Monkey, and Dog by Physiologically Based Pharmacokinetic Model and the Extrapolation to Human. *Front. Pharmacol.* 7, 488. doi:10.3389/fphar.2016.00488
- Drozdziak, M., Gröer, C., Penski, J., Lapczuk, J., Ostrowski, M., Lai, Y., et al. (2014). Protein Abundance of Clinically Relevant Multidrug Transporters along the Entire Length of the Human Intestine. *Mol. Pharm.* 11 (10), 3547–3555. doi:10.1021/mp500330y
- Esumi, Y., Otsuki, T., and Nanpo, T. (1979). Studies on Absorption, Distribution and Excretion of Cefadroxil (Author's Transl). *Jpn. J. Antibiot.* 32 (12), 1350–1355.
- García-Carbonell, M. C., Granero, L., Torres-Molina, F., Aristorena, J. C., Chesa-Jiménez, J., Plá-Delfina, J. M., et al. (1993). Nonlinear Pharmacokinetics of Cefadroxil in the Rat. *Drug Metab. Dispos* 21 (2), 215–217.
- Garrigues, T. M., Martin, U., Peris-Ribera, J. E., and Prescott, L. F. (1991). Dose-dependent Absorption and Elimination of Cefadroxil in Man. *Eur. J. Clin. Pharmacol.* 41 (2), 179–183. doi:10.1007/BF00265914
- Gröer, C., Brück, S., Lai, Y., Paulick, A., Busemann, A., Heidecke, C. D., et al. (2013). LC-MS/MS-based Quantification of Clinically Relevant Intestinal Uptake and Efflux Transporter Proteins. *J. Pharm. Biomed. Anal.* 85, 253–261. doi:10.1016/j.jpba.2013.07.031S0731-7085(13)00337-3
- Hosseini-Yeganeh, M., and McLachlan, A. J. (2002). Physiologically Based Pharmacokinetic Model for Terbinafine in Rats and Humans. *Antimicrob. Agents Chemother.* 46 (7), 2219–2228. doi:10.1128/aac.46.7.2219-2228.2002
- Hu, Y., and Smith, D. E. (2016). Species Differences in the Pharmacokinetics of Cefadroxil as Determined in Wildtype and Humanized PepT1 Mice. *Biochem. Pharmacol.* 107, 81–90. doi:10.1016/j.bcp.2016.03.008S0006-2952(16)00161-1
- Jin, H. E., Kim, I. B., Kim, Y. C., Cho, K. H., and Maeng, H. J. (2014). Determination of Cefadroxil in Rat Plasma and Urine Using LC-MS/MS and its Application to Pharmacokinetic and Urinary Excretion Studies. *J. Chromatogr. B Analyt. Technol. Biomed. Life Sci.* 947–948, 103–110. doi:10.1016/j.jchromb.2013.12.027S1570-0232(13)00716-2
- Jones, H. M., Chen, Y., Gibson, C., Heimbach, T., Parrott, N., Peters, S. A., et al. (2015). Physiologically Based Pharmacokinetic Modeling in Drug Discovery and Development: a Pharmaceutical Industry Perspective. *Clin. Pharmacol. Ther.* 97 (3), 247–262. doi:10.1002/cpt.37
- Kesisoglou, F., Chung, J., van Asperen, J., and Heimbach, T. (2016). Physiologically Based Absorption Modeling to Impact Biopharmaceutics and Formulation Strategies in Drug Development-Industry Case Studies. *J. Pharm. Sci.* 105 (9), 2723–2734. doi:10.1016/j.xphs.2015.11.034
- Kim, Y. C., Kim, I. B., Noh, C. K., Quach, H. P., Yoon, I. S., Chow, E. C. Y., et al. (2014). Effects of 1 $\alpha$ ,25-Dihydroxyvitamin D<sub>3</sub>, the Natural Vitamin D Receptor Ligand, on the Pharmacokinetics of Cefdinir and Cefadroxil, Organic Anion Transporter Substrates, in Rat. *J. Pharm. Sci.* 103 (11), 3793–3805. doi:10.1002/jps.24195
- Kong, W. M., Sun, B. B., Wang, Z. J., Zheng, X. K., Zhao, K. J., Chen, Y., et al. (2020). Physiologically Based Pharmacokinetic-Pharmacodynamic Modeling for Prediction of Vonoprazan Pharmacokinetics and its Inhibition on Gastric Acid Secretion Following Intravenous/oral Administration to Rats, Dogs and Humans. *Acta Pharmacol. Sin* 41 (6), 852–865. doi:10.1038/s41401-019-0353-210.1038/s41401-019-0353-2
- Li, M., Zou, P., Tyner, K., and Lee, S. (2017). Physiologically Based Pharmacokinetic (PBPK) Modeling of Pharmaceutical Nanoparticles. *AAPS J.* 19 (1), 26–42. doi:10.1208/s12248-016-0010-310.1208/s12248-016-0010-3
- Nightingale, C. (1980). Pharmacokinetics of the Oral Cephalosporins in Adults. *J. Int. Med. Res.* 8 (Suppl. 1), 2–8.
- Nightingale, C. H. (1986). Penetration and Concentration of Cefadroxil in Sputum, Lung and Pleural Fluid. *Drugs* 32 (Suppl. 3), 17–20. doi:10.2165/00003495-198600323-00004
- Nungu, K. S., Larsson, S., Wallinder, L., and Holm, S. (1995). Bone and Wound Fluid Concentrations of Cephalosporins. Oral Cefadroxil and Parenteral Cefuroxime Compared in 52 Patients with a Trochanteric Fracture. *Acta Orthop. Scand.* 66 (2), 161–165. doi:10.3109/17453679508995513
- Palmu, A., Jarvinen, H., Hallynck, T., and Pijk, P. J. (1980). Cefadroxil Levels in Bile in Biliary Infections: In Nelson & Grassi (Eds) Chemotherapy and Infectious Disease. *Am. Soc. Microbiol.* 1, 643–644.
- Posada, M. M., and Smith, D. E. (2013a). *In Vivo* Absorption and Disposition of Cefadroxil after Escalating Oral Doses in Wild-type and PepT1 Knockout Mice. *Pharm. Res.* 30 (11), 2931–2939. doi:10.1007/s11095-013-1168-3
- Posada, M. M., and Smith, D. E. (2013b). Relevance of PepT1 in the Intestinal Permeability and Oral Absorption of Cefadroxil. *Pharm. Res.* 30 (4), 1017–1025. doi:10.1007/s11095-012-0937-8
- Poulin, P., and Theil, F. P. (2002). Prediction of Pharmacokinetics Prior to *In Vivo* Studies. II. Generic Physiologically Based Pharmacokinetic Models of Drug Disposition. *J. Pharm. Sci.* 91 (5), 1358–1370. doi:10.1002/jps.10128S0022-3549(16)31006-1
- Rodgers, T., Leahy, D., and Rowland, M. (2005). Physiologically Based Pharmacokinetic Modeling 1: Predicting the Tissue Distribution of Moderate-to-strong Bases. *J. Pharm. Sci.* 94 (6), 1259–1276. doi:10.1002/jps.20322S0022-3549(16)31789-0
- Santella, P. J., and Henness, D. (1982). A Review of the Bioavailability of Cefadroxil. *J. Antimicrob. Chemother.* 10 (Suppl. B), 17–25. doi:10.1093/jac/10.suppl\_b.17
- Shoghi, E., Fuguet, E., Bosch, E., and Ràfols, C. (2013). Solubility-pH Profiles of Some Acidic, Basic and Amphoteric Drugs. *Eur. J. Pharm. Sci.* 48 (1–2), 291–300. doi:10.1016/j.ejps.2012.10.028S0928-0987(12)00431-9
- Simon, C. (1980). Serum and Skin Blister Levels of Cefadroxil in Comparison to Cephalixin. *Infection* 8 (Suppl. 5), 584–587. doi:10.1007/bf01639675
- Sun, L., Wang, C., and Zhang, Y. (2018). A Physiologically Based Pharmacokinetic Model for Valacyclovir Established Based on Absolute Expression Quantity of hPEPT1 and its Application. *Eur. J. Pharm. Sci.* 123, 560–568. doi:10.1016/j.ejps.2018.07.057
- Tanrisever, B., and Santella, P. J. (1986). Cefadroxil. A Review of its Antibacterial, Pharmacokinetic and Therapeutic Properties in Comparison with Cephalixin and Cephhradine. *Drugs* 32 (Suppl. 3), 1–16. doi:10.2165/00003495-198600323-00003
- Xie, Y., Shen, H., Hu, Y., Feng, M. R., and Smith, D. E. (2016). Population Pharmacokinetic Modeling of Cefadroxil Renal Transport in Wild-type and Pept2 Knockout Mice. *Xenobiotica* 46 (4), 342–349. doi:10.3109/00498254.2015.1080881

**Conflict of Interest:** The authors declare that the research was conducted in the absence of any commercial or financial relationships that could be construed as a potential conflict of interest.

**Publisher's Note:** All claims expressed in this article are solely those of the authors and do not necessarily represent those of their affiliated organizations or those of the publisher, the editors, and the reviewers. Any product that may be evaluated in this article, or claim that may be made by its manufacturer, is not guaranteed or endorsed by the publisher.

Copyright © 2021 Tan, Zhang, Wang and Sun. This is an open-access article distributed under the terms of the Creative Commons Attribution License (CC BY). The use, distribution or reproduction in other forums is permitted, provided the original author(s) and the copyright owner(s) are credited and that the original publication in this journal is cited, in accordance with accepted academic practice. No use, distribution or reproduction is permitted which does not comply with these terms.